CONDENSED MATTER PHYSICS

Impact of surface roughness on liquid-liquid transition

Ken-ichiro Murata* and Hajime Tanaka†

Liquid-liquid transition (LLT) in single-component liquids is one of the most mysterious phenomena in condensed matter. So far, this problem has attracted attention mainly from the fundamental viewpoint. We report the first experimental study on an impact of surface nanostructuring on LLT by using a surface treatment called rubbing, which is the key technology for the production of liquid crystal displays. We find that this rubbing treatment has a significant impact on the kinetics of LLT of an isotropic molecular liquid, triphenyl phosphite. For a liquid confined between rubbed surfaces, surface-induced barrierless formation of the liquid II phase is observed even in a metastable state, where there should be a barrier for nucleation of the liquid II phase in bulk. Thus, surface rubbing of substrates not only changes the ordering behavior but also significantly accelerates the kinetics. This spatiotemporal pattern modulation of LLT can be explained by a wedge-filling transition and the resulting drastic reduction of the nucleation barrier. However, this effect completely disappears in the unstable (spinodal) regime, indicating the absence of the activation barrier even for bulk LLT. This confirms the presence of nucleation-growth– and spinodal decomposition–type LLT, supporting the conclusion that LLT is truly a first-order transition with criticality. Our finding also opens up a new way to control the kinetics of LLT of a liquid confined in a solid cell by structuring its surface on a mesoscopic length scale, which may contribute to making LLT useful for microfluidics and other industrial applications.

INTRODUCTION

Generally, surface wettability and geometry seriously affect a phase transition near a surface through a coupling of the surface field to the order-parameter field. This leads to unique phenomena absent in bulk (1–4). Such examples can be seen for crystallization, vapor-liquid phase transition (5), and phase separation of a binary mixture (6) in contact with a substrate. Heterogeneous nucleation (that is, preferential nucleation on a wettable surface) is one of such classical examples widely seen in our daily lives, ranging from cloud and frost formation in nature to the production of high-quality single crystals in industry. These phenomena should not be regarded as a special exception to bulk phase transition because it is almost impossible to avoid the presence of surfaces in any real systems, particularly, in small-size systems relevant to nanotechnology applications. Recently, there have been growing interests in controlling self-organized pattern evolution by nanostructured functional surfaces using an interplay between phase ordering and wetting (4–9).

Here, we focus our attention on how substrate surface geometries affect liquid-liquid transition (LLT) of a single-component liquid, which is the first-order phase transition between two liquid states, liquids I and II. Recently, LLT has attracted considerable attention because of its counterintuitive nature (10–13). LLT accompanies distinct changes of bulk physical and chemical properties such as density (14), refractive index (14, 15), dielectric constant (16, 17), polarity (18), viscosity (15), fragility (19), and miscibility (20). Controlling these properties while maintaining fluidity can be important for practical applications of LLT because the state of a liquid is key to various transport and chemical reaction processes. LLT offers an intriguing possibility to change the physical and chemical properties of a liquid without modifying its molecular structure. In addition to the change in these bulk properties, we recently found a difference in the wettability between liquids I and II of triphenyl phosphite to a solid substrate (21), suggesting a possibility of controlling LLT by a surface field. There has been a long-standing debate on the physical nature of the phase transition in triphenyl phosphite (16, 22–34) since its first observation by Cohen et al. (14) and Ha et al. (14, 35). The difficulty comes from the fact that the transition takes place below the melting point, that is, in a state intrinsically metastable against crystallization. However, recent experimental studies (18, 36–38) have shown that the transition is LLT and not merely due to nanocrystal formation.

LLT looks counterintuitive if we assume that a liquid has a completely random structure. However, LLT can be naturally explained by introducing a new additional scalar order parameter (39–42) in addition to density ρ, a standard order parameter describing the liquid state. We argued that this new order parameter should be the fraction of locally favored structures, S. Although ρ is a conserved order parameter, S is a nonconserved one because locally favored structures can be created and independently annihilated, as spin flipping in magnets. This explains why liquid I completely transforms into liquid II without coexistence, unlike phase separation of a mixture. Then, LLT is regarded as a gas-liquid–like cooperative ordering of locally favored structures: Liquids I and II are a gas (dilute) and a liquid (dense) state of locally favored structures, respectively. Thus, the transformation from liquid I to II is the process of the increase in the fraction of locally favored structures (37). In this scenario, a gas-liquid transition is dominated by ρ, whereas an LLT is dominated by S.

Here, we report the first experimental study on an impact of surface nanostructuring on LLT. By comparing the ordering process of LLT of triphenyl phosphite in contact with rubbed substrates to that with unrubbed smooth ones for both nucleation-growth (NG)– and spinodal decomposition (SD)–type LLT, we find that surface structuring by rubbing, which is widely used in liquid-crystal industries, strongly accelerates the kinetics of NG-type LLT. We show that rubbing significantly affects the pattern formation and accelerates the kinetics for NG-type LLT but has no effects on SD-type LLT. This sheds new light on the very nature of LLT. Furthermore, this controllability of the kinetics of LLT by wedge-wetting effects will open a new avenue of LLT research toward microfluidics and other industrial applications.

Department of Fundamental Engineering, Institute of Industrial Science, University of Tokyo, 4-6-1 Komaba, Meguro-ku, Tokyo 153-8505, Japan.
*Present address: Institute of Low Temperature Science, Hokkaido University, Kita-19, Nishi-8, Kita-ku, Sapporo 060-0819, Japan.
†Corresponding author. Email: tanaka@iis.u-tokyo.ac.jp

RESULTS AND DISCUSSION

Rubbing effects on NG-type LLT

First, we show (in Fig. 1A) a typical pattern evolution process of LLT in a cell made of unrubbed planar surfaces, which was observed with phase-contrast microscopy at the annealing temperature T_a = 218 K (see movie S1). This temperature is located in the metastable region of LLT or below the binodal temperature T_{BN} but above the spinodal temperature T_{SD} = 215.5 K. In an unrubbed cell, spherical droplets of liquid II are nucleated, increase their size linearly with time in the matrix of liquid I, and, finally, fill up an entire space. The schematic explanation of NG-type pattern evolution in a system confined between two solid substrates is also shown in Fig. 1A. On the other hand, in a rubbed cell, whose surfaces have plenty of submicrometer-scale grooves formed along the rubbing direction (white arrow), barrierless formation of liquid II domains is observed (see Fig. 1B and movie S2). In this case, LLT is initiated by the barrierless formation of liquid II domains on the rubbed substrates, which is followed by the growth toward the middle of the cell, resulting in the gradual increase of the intensity of the image with time. This is unlike in the above case of typical NG-type pattern evolution, where dark droplets of liquid II are directly formed in the middle of the matrix of liquid I (see schematic pictures in Fig. 1). As shown below, this leads to a difference in the temporal change in the intensity distribution (see Fig. 2). This behavior is fundamentally different from the ordinary NG-type transformation shown in Fig. 1A, despite the fact that both processes take place at thermodynamically identical conditions. However, even in Fig. 1B, we can see the nucleation of dark droplets (see, for example, encircled area) in the intermediate stage of the process in addition to the pattern formed near the surfaces. We found that these dark droplets of liquid II do not appear for a cell whose thickness is less than 5 µm. Together with microscopy observations with different focal depths, we conclude that nucleation of dark liquid II droplets overcoming a barrier takes place in the middle (bulk) part of the cell after the surface-assisted barrierless formation of the liquid II domains takes place (see schematic in Fig. 1A). We note that in the later stage, these droplets are merged with the liquid II wetting layers formed on the walls, which propagate from the surfaces toward the middle of the cell and thus eventually merge with the droplets. We confirm that the surface effects are significant, at least for a cell thickness less than a few tens of micrometers.

We also measured the temporal change in the intensity distribution $P(I)$ of a microscopy image, which is proportional to the density distribution $P(\rho)$. Note that phase-contrast microscopy detects the difference in the refractive index, which is proportional to the density difference: A darker contrast means a higher density in our measurements (43). Because the locally favored structure has a higher density than the normal liquid structure, $P(\rho)$ reflects $P(S)$. As shown in Fig. 2A, the temporal change of $P(I)$ for the unrubbed cell (see Fig. 1A) is identical to that of our previous study (44): Right large and left small peaks corresponding to liquid I (bright matrix region) and liquid II (dark droplets), respectively, coexist in the intermediate stage of LLT, which is characteristic of NG-type transformation. It is well known that, in NG-type ordering, nuclei with the final order-parameter value (forming the peak of low intensity in this case) appear in the majority matrix (forming the peak of high intensity), and the peak of nuclei grows without a big change in the peak position (or the order-parameter value).
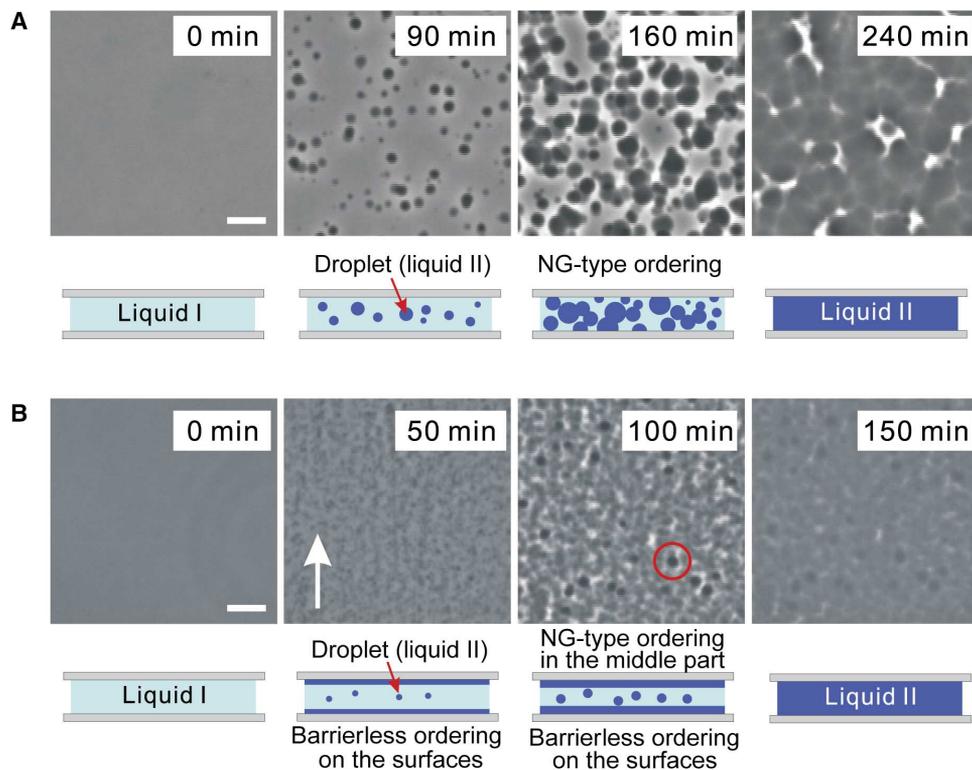
Fig. 1. Comparison of pattern evolution between LLT on smooth unrubbed and rubbed surfaces. Pattern evolution observed at T_a = 218 K in an unrubbed smooth (**A**) and a rubbed (**B**) cell with phase-contrast microscopy. The pattern formation process can also be seen in movies S1 and S2 for (A) and (B), respectively. The cell thickness is 10 µm for both cases. Scale bars, 20 µm. Schematics illustrate cross-sectional views of the ordering processes.
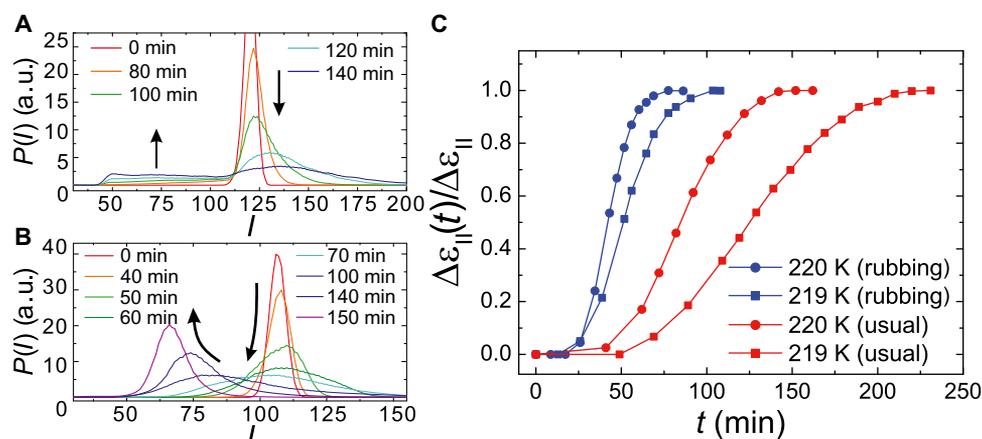
Fig. 2. Dynamic acceleration of LLT on rubbed surfaces relative to that on unrubbed ones. Temporal change of $P(I)$ during LLT at $T_a = 218$ K for a smooth (**A**) and a rubbed (**B**) cell. a.u., arbitrary units. (**C**) Time evolution of the normalized dielectric relaxation strength of liquid II, $\Delta\varepsilon_{II}(t)/\Delta\varepsilon_{II}$, at $T_a = 219$ K (squares) and 220 K (circles) for rubbed (blue) and unrubbed (red) cells. It is found that, for both temperatures, the evolution of $\Delta\varepsilon_{II}$ becomes two or three times faster in rubbed cells than in usual cells.

Here, we note that the left small peak is very broad due to a focal depth problem (see the Supplementary Materials for details). In contrast, $P(I)$ for the rubbed cell (see Fig. 1B) does not have a bimodal-like shape but rather broadens while continuously changing its peak position from the right peak of liquid I to the left peak of liquid II without creating another peak (see Fig. 2B). In the rubbed cell, the growth of the liquid II phase is not limited by the nucleation process, because there is no barrier for its formation, but mainly by the growth process toward the middle of the cell. Thus, the continuous increase of the wetting layer thickness is the origin of the continuous shift of the peak intensity (see the schematic in Fig. 1B). This temporal change of $P(I)$ is reminiscent of the behavior of SD-type LLT (44). This similarity comes from the barrierless formation of the liquid II phase, but, at the same time, there is a crucial difference in the origin of the continuous change in the peak intensity: For ordinary SD-type LLT, the order parameter itself changes continuously with time, whereas in the above case, the continuous nature comes from the fact that the intensity is proportional to the thickness of the wetting layer, which increases continuously with time. Note that the intensity of the image is the integration along the thickness direction. Furthermore, by comparing Fig. 1 (A and B), we can clearly see that not only the spatial pattern but also the kinetics of LLT are significantly accelerated by surface rubbing due to the barrierless ordering.

To see this more quantitatively, we performed dielectric spectroscopy measurements and evaluated the time evolution of the normalized dielectric strength of liquid II, $\Delta\varepsilon_{II}(t)/\Delta\varepsilon_{II}$, which is a measure of the degree of the transformation from liquid I to liquid II. Figure 2C shows the time evolution of $\Delta\varepsilon_{II}(t)/\Delta\varepsilon_{II}$ at $T_a = 219$ and 220 K for a sample sandwiched between rubbed substrates together with that between unrubbed smooth ones. We found that, for both temperatures, the growth of $\Delta\varepsilon_{II}(t)/\Delta\varepsilon_{II}$ in the rubbed cell is accelerated two- or three-fold compared to that in the unrubbed one. As will be discussed below, LLT in a rubbed cell proceeds as if there is no activation barrier even in a metastable state above T_{SD}. Because the thermodynamic condition is identical and, accordingly, the structural relaxation time is the same between the two cases, the growth kinetics of the order parameter should also be the same. Thus, we conclude that the dynamical acceleration of LLT is a consequence of the absence of the activation barrier for nucleation of liquid II droplets on rubbed sur-

faces: Surface rubbing induces spontaneous barrierless growth of the order parameter even in a metastable state of the bulk liquid.

Origin of rubbing-induced acceleration of NG-type LLT

Next, we consider the physical origin of the spatiotemporal modulation of LLT induced by rubbing. Figure 3A shows a confocal microscopy image of a rubbed substrate. We confirmed a large number of microgrooves aligned along the rubbing direction, with typical intervals of a few micrometers. Figure 3B shows a transient spatial pattern of LLT at $T_a = 220$ K. There, we can see complete filling of the microgrooves by liquid II as well as partial filling by liquid II droplets on aligned microgrooves, which is the origin of the anisotropy in the two-dimensional (2D) power spectrum pattern [identical to the light-scattering pattern (45)], as shown in Fig. 3C. We can see a bright line at $q_x = 0$ in addition to the ordinary isotropic spinodal pattern, indicating the presence of nearly 1D liquid II domains along the rubbed direction (or, on the microgrooves).

The ordering behavior of liquid II on a rubbed substrate is reminiscent of the so-called wedge filling of a liquid (46), provided that a microgroove can be regarded as a wedge. The wetting morphology for a wedge is classified into three types in terms of the relation between the contact angle to the surface (θ) and the wedge angle (α) (47): For $\theta < 90° - \alpha/2$, a liquid completely fills the wedge with a negative Laplace pressure. For $90° - \alpha/2 < \theta < 90° + \alpha/2$, a liquid partially fills the wedge in a droplet-like form with a positive Laplace pressure. For $\theta > 90° + \alpha/2$, no wedge filling takes place. The last condition is satisfied for a water/glycerol mixture, which also exhibits LLT (17). For this system, we did not see any indication of surface-assisted modulation of LLT but only observed a usual NG-type process similar to that in Fig. 1A. This difference in the behavior between triphenyl phosphite and a water/glycerol mixture is a consequence of the rather low wettability of liquid II of the latter to the glass substrate compared to that of the former.

Our two-order–parameter model of liquids (39–41) suggests that there should be a similarity in the pattern evolution between LLT influenced by a rubbed surface and a gas-liquid phase transition under the influence of wedge filling (see Introduction) (5, 9, 47). We recently demonstrated that, in the process of LLT of triphenyl phosphite in contact with a solid wall, a transition from partial to complete wetting
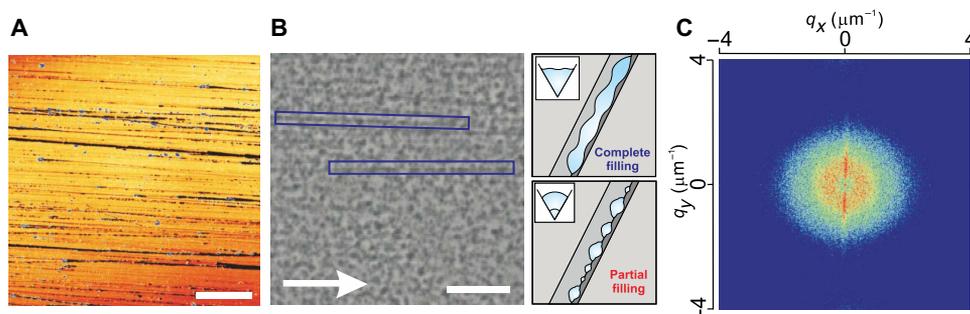
Fig. 3. Anisotropic wetting morphologies induced by rubbing. (**A**) A confocal micrograph of the 10× rubbed substrate. The color in the image corresponds to the height level: The planar area appears yellow. Black indicates height lower than the planar surface, corresponding to scratches (grooves) formed by rubbing, whereas blue indicates height higher than the planar surface, corresponding to ridges or impurities on the substrate. Note that the depth of the microgrooves is less than the resolution of optical and phase-contrast microscopy. Because of the random nature of grooves, their precise characterization by AFM was difficult. (**B**) A transient pattern observed with phase-contrast microscopy during LLT on the 10× rubbed substrate at T_a = 220 K. The white arrow indicates the rubbing direction (that is, the x direction). The complete filling of a wedge by liquid II appears as a filament-like shape (regions enclosed by the blue rectangles), whose situation is depicted in the upper right schematic. In addition, the partial filling by liquid II, whose situation is depicted in the lower right schematic, is also observed. Such coexistence of various wetting patterns may be a consequence of distributions of the wedge angle, depth, and length of grooves formed by rubbing. (**C**) A 2D power spectrum pattern of the image in (B) [see Tanaka et al. (45) for the calculation method]. Scale bars, 50 μm (A and B).

of liquid II takes place on an unrubbed planar substrate when approaching T_{SD} (21), which is reminiscent of "critical point wetting" near a gas-liquid critical point (1, 3). As schematically shown in Fig. 4, the decrease of θ near T_{SD} and T_W should also lead to a transition from partial to complete filling (wedge-filling transition) at a filling temperature T_F, which satisfies θ(T_F) = 90° − α/2. We confirmed that this transition takes place around 220 K: T_F ≈ 220 K (see movie S3). Note that the distributions (or the randomness) of both the wedge angle and the length of the microgrooves produced by rubbing may make the transition rather broad.

Nucleation of droplets basically proceeds with the formation of a new interface between liquids I and II, whose profile is determined to locally minimize the free energy (48). For a system satisfying the filling condition ($T < T_F$ or θ < 90° − α/2), liquid II droplets nucleate and grow while filling a wedge in liquid I. On the other hand, in the critical regime ($T ≈ T_F$ or θ ≈ 90° − α/2), nucleation of liquid II on a wedge is expected to accompany contact-line fluctuations induced by critical wedge filling. Furthermore, the kinetics of LLT on rubbed substrates are distinct from the usual NG-type transformation, which is the activation process overcoming a free-energy barrier associated with the formation of a new interface. For α/2 ≤ 90° − θ, such a barrier for the formation of a new phase vanishes selectively on wedges, leading to a situation similar to the formation of a new phase on a complete wettable surface. Then, the formation of liquid II on a rubbed substrate should proceed spontaneously without an activation barrier, despite the fact that the system is still in a thermodynamically metastable state and not in an unstable state (above T_{SD}). We argue that this is the origin for the kinetic acceleration of LLT in a rubbed cell (see Fig. 2C). We tried to obtain the detailed geometrical characteristics of the surface pattern produced by rubbing with atomic force microscopy (AFM). However, it was difficult to characterize the angle α because of the random nature of rubbed surfaces and artifacts coming from the shape of the probe of AFM (see the Supplementary Materials). To make a quantitative check, we would need to use well-controlled surface structures as done by Seemann et al. (49), which remains a potential area of future research.

Rubbing effects on SD-type LLT

Finally, we consider wedge-wetting effects on SD-type LLT. Figure 5A shows a spatial pattern evolution process of SD-type transformation
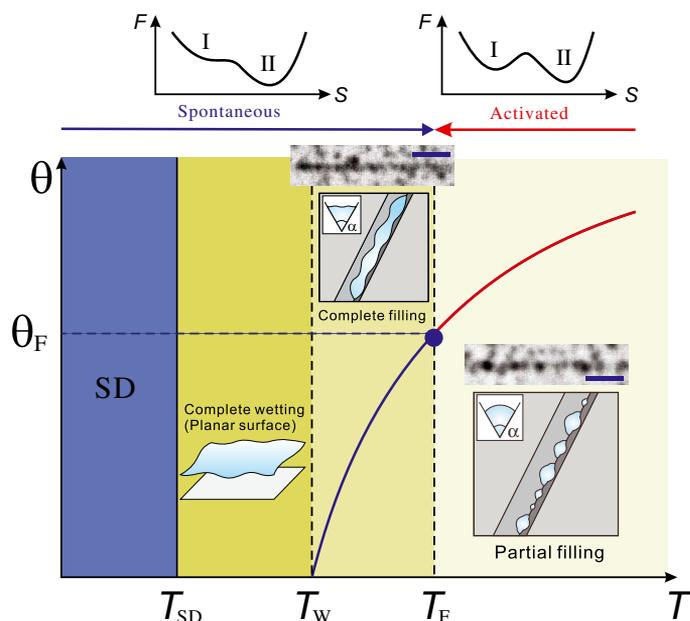
Fig. 4. Relationship between the wedge-filling transition, wetting transition, and spinodal point of LLT. In the top row, we show schematics of the free energy F for two situations, where liquid I is unstable (left) and metastable (right) against liquid II. In our system, the contact angle of liquid II decreases toward zero when approaching T_{SD} because the interfacial tension vanishes toward T_{SD} = 215.5 K (21). Thus, a transition from partial to complete wetting (wetting transition) takes place at the wetting temperature T_W above T_{SD}. For a wedge whose angle is α, the decrease of θ near T_{SD} and T_W also induces a transition from partial to complete filling (wedge-filling transition) at the filling temperature T_F, where the condition θ(T_F) = 90° − α is satisfied. The two phase-contrast microscopy images indicate the formation of the liquid II phase on a well-developed wedge at 218 and 220 K, respectively. Scale bars, 10 μm. Partially filled liquid II begins to appear in the form of droplets above 220 K. The filling temperature T_F of our system is thus considered to be located around 220 K. Note that, in the rubbed cell we used, the surface of the substrate was coated by polyimide, whose contact angle was estimated as 81° at 220 K from our previous study (21). The wedge angle of the microgrooves is thus estimated as 9°. Because of the high contact angle, T_W is expected to be located near the spinodal temperature T_{SD}, that is, T_W ≈ T_{SD}, which makes it very difficult to experimentally determine the wetting transition T_W on a planar polyimide surface.
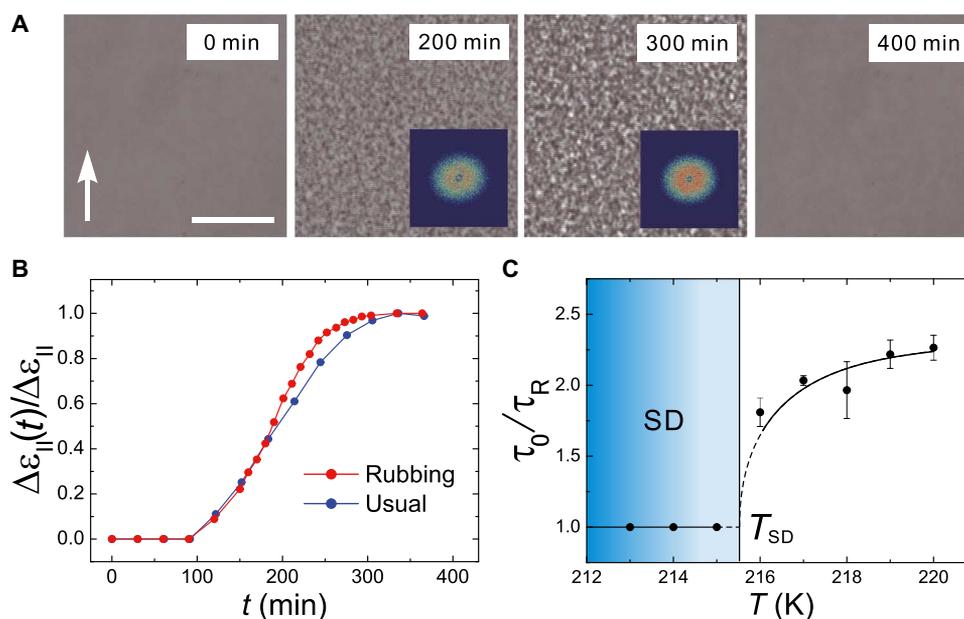
Fig. 5. Pattern evolution during SD-type LLT on a rubbed substrate. (**A**) Pattern evolution observed with phase-contrast microscopy at T_a = 214 K. We observed the initial growth of the amplitude of the order-parameter (S) fluctuations through its coupling to the density (at 200 min) and its coarsening in the later stage (at 300 and 400 min) during LLT. This pattern evolution is identical to that of typical SD-type LLT in triphenyl phosphite (*15, 44*). The white arrow indicates the rubbing direction. Scale bar, 50 μm. Insets (at 200 and 300 min) are 2D power spectrum images obtained by digital image analysis (*40*), which is isotropic, unlike in the case of NG-type LLT (see Fig. 3C). (**B**) A direct comparison of $\Delta\varepsilon_\parallel(t)/\Delta\varepsilon_\parallel$ at T_a = 214 K between the rubbed and smooth unrubbed surface case. (**C**) Temperature dependence of the ratio of the incubation time of LLT between the rubbed surface case (τ_R) and the smooth unrubbed surface case (τ_0). We define τ_R and τ_0 as the time when an SD-like pattern appears on the surface and when the area fraction of droplets of liquid II in liquid I matrix reaches 0.02, respectively. LLT on the rubbed surface proceeds spontaneously without an activation energy below T_F, whereas LLT in bulk does so only below T_{SD}. Above T_{SD}, LLT in the unrubbed surface case (or in bulk) proceeds by overcoming an activation barrier required for nucleation of liquid I droplets.

on a rubbed surface at 214 K. We also show a direct comparison of the evolution of $\Delta\varepsilon_\parallel$ between a rubbed and an unrubbed cell in Fig. 5B. Unlike the NG case, there are no effects of rubbing on pattern evolution. The patterns are isotropic (see also the isotropic 2D power spectrum images shown in the insets of Fig. 5A), and there is no kinetic acceleration. This behavior is fully consistent with our previous observation that surface-wetting effects have no impact on SD-type LLT even for a complete wetting surface (*21*). The absence of wedge- and surface-wetting effects is a direct consequence of (i) the short-range nature of the surface field (*21*) and (ii) the nonconserved nature of the order parameter (*40*). The former leads to an extremely slow growth of wetting (or filling) layer ($\sim \ln t$) for an unstable regime (*50*) compared to bulk coarsening. Thus, fast-growing fluctuations in bulk overwhelm slowly growing wetting layers. This is because the latter allows only a local change of the order parameter near the surface and thus cannot be delocalized because of the irrelevance of diffusion and/or flow unlike in a system of a conserved order parameter (*51*). This is a consequence of the nonconserved nature of the order parameter, which can change locally without accompanying diffusion. On the other hand, for a system of a conserved order parameter (for example, phase separation of a binary mixture and a vapor-liquid transition), wedge-wetting effects are expected to have a serious influence on the kinetics of SD-type transformation via surface-induced composition waves and interfacial tension–driven flow, reflecting its nonlocal nature (*51*).

We have shown that the effects of rubbing on LLT are significantly different between below T_{SD} and above T_{SD}. Figure 5C shows the ratio of the incubation time of LLT in an unrubbed cell (τ_0) to that in a rubbed cell (τ_R) below T_F. Here, we independently determine the spi-

nodal point T_{SD} by optical microscopy measurements (vertical dashed lines) (*15*). Although the accuracy of the determination of the ratio τ_0/τ_R is not remarkably high (see error bars in Fig. 5C), we can see that, by decreasing the temperature, τ_0/τ_R drastically decreases toward T_{SD} in the metastable (NG) region and then becomes a constant ($\tau_0/\tau_R = 1$) in the unstable (SD) region, which means that there is no kinetic acceleration below T_{SD}. This strongly supports the scenario described above. The relation $\tau_0/\tau_R = 1$ suggests that the bulk growth is dominant even in a rubbed cell below T_{SD} (see above). Note that as the system approaches T_{SD}, the nucleation barrier for liquid II droplets decreases, and thus, rubbing effects gradually become less important. Accordingly, the difference in the kinetics between the rubbed and unrubbed cases gradually becomes smaller toward T_{SD} and finally disappears completely at T_{SD}.

CONCLUSION

In conclusion, we have demonstrated that the spatiotemporal pattern evolution of NG-type LLT in triphenyl phosphite is seriously influenced by surface rubbing, which induces a wedge-filling transition. Even in a metastable region, rubbing induces spontaneous barrierless transformation from liquid I to liquid II on the substrates and thus significantly accelerates the kinetics of LLT. We also show that the absence of wedge-wetting effects on the kinetics of SD-type LLT is unique to the ordering governed by a nonconserved order parameter. We note that this is markedly different from a system of a conserved order parameter (for example, a binary liquid mixture), where surface-wetting effects seriously affect the pattern evolution of SD and accelerate the kinetics via diffusion or hydrodynamic flow (*51*).

Furthermore, the disappearance of wedge-wetting effects below the spinodal temperature T_{SD} strongly suggests that there is no activation barrier for the transformation of liquid I to liquid II below T_{SD}. That is, the transition mode in fact changes from NG-type (metastable) to SD-type (unstable) LLT at T_{SD}. The presence of SD-type ordering further supports that the transition is primarily LLT and "not" nano-crystal formation [see also recent research (18, 36–38, 41, 42) and references therein]. As mentioned above, the behavior also indicates that the order parameter governing the LLT is of a nonconserved nature. These findings shed new light on the physical nature of LLT, including the characterization of the nature of the order parameter governing it.

Finally, from an applications viewpoint, our finding may open up a previously unreported way to control the kinetics of LLT in a metastable state, which leads to a change in liquid properties (such as density, refractive index, chemical properties, and transport properties), by using surface structuring of a container. Such surface effects should be particularly important for nano- and microfluidic applications. Furthermore, the development of surface fabrication techniques capable of providing designed nanostructures would offer more accurate spatiotemporal control of LLT.

MATERIALS AND METHODS
Experimental details
The sample used in this study is triphenyl phosphite, which was purchased from Acros Organics. We used it after extracting only a crystallizable part to remove impurities. We carefully avoided moisture by using dried nitrogen gas in order to prevent chemical decomposition of triphenyl phosphite because the molecules are known to decompose under the presence of water due to ester hydrolysis. The temperature was controlled within ±0.1 K by a computer-controlled hot stage (LK-600PH; Linkam Scientific) with a cooling unit (L-600A; Linkam Scientific). Sample cells used in this measurement, which were composed of two parallel glass substrates coated with 3× or 10× rubbed polyimide (rubbed cells) and with an unrubbed polyimide (usual cells), were purchased from E.H.C. Co. Ltd. For the rubbed cells, both top and bottom surfaces were rubbed along the same direction. We used a Leica SP5 confocal microscope to measure a surface roughness pattern of the rubbed substrate. An indium tin oxide transparent electrode was also deposited on the glass substrate, which allowed us to simultaneously perform dielectric spectroscopy measurements and microscopy observation. Here, the transparent electrode had no effect on the wetting dynamics of LLT because polyimide was further coated on the electrodes. The cell thickness was fixed to 5 or 10 μm, with an error of ±1 μm. We observed a transformation process from liquid I to liquid II with phase-contrast microscopy (BH2-UMA; Olympus). Broadband dielectric measurements were performed in a frequency range of 10 mHz to 1 MHz with an Impedance/Gain-Phase Analyzer (Solartron SI 1260).

SUPPLEMENTARY MATERIALS
Supplementary material for this article is available at http://advances.sciencemag.org/cgi/content/full/3/2/e1602209/DC1
section S1. The shape of the intensity distribution function $P(I)$
section S2. The AFM observation of the rubbed substrate
fig. S1. Relation between a phase-contrast image and the intensity distribution function.
fig. S2. AFM image of the rubbed surface.
movie S1. LLT in the smooth unrubbed cell observed at 218 K (the same process as Fig. 1A).
movie S2. LLT in the rubbed cell observed at 218 K (the same process as Fig. 1B).
movie S3. LLT in the rubbed cell at four different temperatures.

REFERENCES AND NOTES
1. J. W. Cahn, Critical point wetting. *J. Chem. Phys.* **66**, 3667–3672 (1977).
2. P. G. de Gennes, Wetting: Statics and dynamics. *Rev. Mod. Phys.* **57**, 827–863 (1985).
3. D. Bonn, D. Ross, Wetting transitions. *Rep. Prog. Phys.* **64**, 1085–1163 (2001).
4. M. Rauscher, S. Dietrich, Wetting phenomena in nanofluidics. *Annu. Rev. Mater. Res.* **38**, 143–172 (2008).
5. C. Rascón, A. O. Parry, Geometry-dominated fluid adsorption on sculpted solid substrates. *Nature* **407**, 986–989 (2000).
6. M. Böltau, S. Walheim, J. Mlynek, G. Krausch, U. Steiner, Surface-induced structure formation of polymer blends on patterned substrates. *Nature* **391**, 877–879 (1998).
7. H. Gau, S. Herminghaus, P. Lenz, R. Lipowsky, Liquid morphologies on structured surface: From microchannels to microchips. *Science* **283**, 46–49 (1999).
8. A. M. Higgins, R. A. L. Jones, Anistropic spinodal dewetting as a route to self-assembly of patterned surfaces. *Nature* **404**, 476–478 (2000).
9. S. Herminghaus, M. Brinkmann, R. Seemann, Wetting and dewetting of complex surface geometries. *Annu. Rev. Mater. Res.* **38**, 101–121 (2008).
10. O. Mishima, H. E. Stanley, The relationship between liquid, supercooled and glassy water. *Nature* **396**, 329–335 (1998).
11. Y. Katayama, T. Mizutani, W. Utsumi, O. Shimomura, M. Yamakata, K.-i. Funakosi, A first-order liquid-liquid transition in phosphorus. *Nature* **403**, 170–173 (2000).
12. S. Aasland, P. F. McMillan, Density-driven liquid–liquid phase-separation in the system Al_2O_3–Y_2O_3. *Nature* **369**, 633–636 (1994).
13. S. Sastry, C. A. Angell, Liquid-liquid phase transition in supercooled silicon. *Nat. Mater.* **2**, 739–743 (2003).
14. I. Cohen, A. Ha, X. Zhao, M. Lee, T. Fisher, M. J. Strouse, D. Kivelson, A low-temperature amorphous phase in fragile glass-forming substance. *J. Phys. Chem.* **100**, 8518–8526 (1996).
15. H. Tanaka, R. Kurita, H. Mataki, Liquid-liquid transition in the molecular liquid triphenyl phosphite. *Phys. Rev. Lett.* **92**, 025701 (2004).
16. S. Dvinskikh, G. Benini, J. Senker, M. Vogel, J. Wiedersich, A. Kudlik, E. Rössler, Molecular motion in the two amorphous phases of triphenyl phosphite. *J. Phys. Chem. B* **103**, 1727–1737 (1999).
17. K. Murata, H. Tanaka, Liquid–liquid transition without macroscopic phase separation in a water–glycerol mixture. *Nat. Mater.* **11**, 436–443 (2012).
18. J. Mosses, C. D. Syme, K. Wynne, The order parameter of the liquid-liquid transition in a molecular liquid. *J. Phys. Chem. Lett.* **6**, 38–43 (2014).
19. R. Kurita, H. Tanaka, Control of the fragility of a glass-forming liquid using the liquid-liquid phase transition. *Phys. Rev. Lett.* **95**, 065701 (2005).
20. R. Kurita, K. Murata, H. Tanaka, Control of fluidity and miscibility of a binary liquid mixture by the liquid-liquid transition. *Nat. Mater.* **7**, 647–652 (2008).
21. K. Murata, H. Tanaka, Surface-wetting effects on the liquid–liquid transition of a single-component molecular liquid. *Nat. Commun.* **1**, 16 (2010).
22. G. P. Johari, C. Ferrari, Calorimetric and dielectric investigations of the phase transformations and glass transition of triphenyl phosphite. *J. Phys. Chem. B* **101**, 10191–10197 (1997).
23. A. Hédoux, Y. Guinet, M. Descamps, Raman signature of polyamorphsim in triphenyl phosphite. *Phys. Rev. B* **58**, 31–34 (1998).
24. A. Hédoux, O. Hernandez, J. Lefebvre, Y. Guinet, M. Descamps, Mesoscopic description of the glacial state in triphenyl phosphite from x-ray diffraction experiment. *Phys. Rev. B* **60**, 9390–9395 (1999).
25. A. Hédoux, P. Derollez, Y. Guinet, A. J. Dianoux, M. Descamps, Low-frequency vibrational excitations in the amorphous and crystalline states of triphenyl phosphite: A neutron and Raman scattering investigation. *Phys. Rev. B* **63**, 144202–144207 (2001).
26. A. Hédoux, J. Dore, Y. Guinet, M. C. Bellissent-Funel, D. Prevost, M. Descamps, D. Grandjean, Analysis of the local order in the glacial state of triphenyl phosphite by neutron diffraction. *Phys. Chem. Chem. Phys.* **4**, 5644–5648 (2002).
27. M. Mizukami, K. Kobashi, M. Hanaya, M. Oguni, Presence of two freezing-in processes concerning α-glass transition in the new liquid triphenyl phosphite and its consistency with "cluster structure" and "intracluster rearrangement for α process" models. *J. Phys. Chem. B* **103**, 4078–4088 (1999).
28. C. Alba-Simionesco, G. Tarjus, Experimental evidence of mesoscopic order in the apparently amorphous glacial phase of the fragile glass former triphenyl phosphite. *Europhys. Lett.* **52**, 297–303 (2000).
29. Q. Mei, P. Ghalsasi, C. J. Benmore, J. L. Yager, The local structure of triphenyl phosphite studied using spallation neutron and high-energy X-ray diffraction. *J. Phys. Chem. B* **108**, 20076–20082 (2004).
30. Q. Mei, J. E. Siewenie, C. J. Benmore, P. Ghalsasi, J. L. Yarger, Orientational correlations in the glacial state of triphenyl phosphite. *J. Phys. Chem. B* **110**, 9747–9750 (2006).

31. B. E. Schwickert, S. R. Kline, H. Zimmermann, K. M. Lantzky, J. L. Yarger, Early stages glacial clustering in supercooled triphenyl phosphite. *Phys. Rev. B* **64**, 045410 (2001).

32. J. Senker, J. Sehnert, S. Correll, Microscopic description of the polyamorphic phases of triphenyl phosphite by means of multidimensional solid-state NMR spectroscopy. *J. Am. Chem. Soc.* **127**, 337–349 (2005).

33. O. Hernandez, A. Hédoux, J. Lefevbre, Y. Guinet, M. Descamps, R. Papoular, O. Masson, *Ab initio* structure determination of triphenyl phosphite by powder synchrotron X-ray diffraction. *J. Appl. Crystallogr.* **35**, 212–219 (2002).

34. O. J. Hernandez, A. Boucekkine, A. Hédoux, Density functional theory study of triphenyl phosphite: Molecular flexibility and weak intermolecular hydrogen bonding. *J. Phys. Chem. A* **111**, 6952–6958 (2007).

35. A. Ha, I. Cohen, X. Zhao, M. Lee, D. Kivelson, Supercooled liquids and polyamorphism. *J. Phys. Chem.* **100**, 1–4 (1996).

36. R. Shimizu, M. Kobayashi, H. Tanaka, Evidence of liquid-liquid transition in triphenyl phosphite from time-resolved light scattering experiments. *Phys. Rev. Lett.* **112**, 125702 (2014).

37. K. Murata, H. Tanaka, Microscopic identification of the order parameter governing liquid-liquid transition in a molecular liquid. *Proc. Natl. Acad. Sci. U.S.A.* **112**, 5956–5961 (2015).

38. M. Kobayashi, H. Tanaka, The reversibility and first-order nature of liquid–liquid transition in a molecular liquid. *Nat. Commun.* **7**, 13438 (2016).

39. H. Tanaka, A simple physical model of liquid-glass transition: Intrinsic fluctuating interactions and random fields hidden in glass-forming liquids. *J. Phys. Condens. Matter* **10**, L207–L214 (1998).

40. H. Tanaka, General view of a liquid-liquid phase transition. *Phys. Rev. E* **62**, 6968–6976 (2000).

41. H. Tanaka, Bond orientational order in liquids: Towards a unified description of water-like anomalies, liquid-liquid transition, glass transition, and crystallization. *Eur. Phys. J. E* **35**, 113–196 (2012).

42. H. Tanaka, Importance of many-body orientational correlations in the physical description of liquids. *Faraday Discuss.* **167**, 9–76 (2013).

43. H. Tanaka, T. Nishi, Direct determination of the probability distribution function of concentration in polymer mixtures undergoing phase separation. *Phys. Rev. Lett.* **59**, 692–695 (1987).

44. R. Kurita, H. Tanaka, Critical-like phenomena associated with liquid-liquid transition in a molecular liquid. *Science* **306**, 845–848 (2004).

45. H. Tanaka, T. Hayashi, T. Nishi, Application of digital image analysis to pattern formation in polymer systems. *J. Appl. Phys.* **59**, 3627–3643 (1986).

46. A. O. Parry, A. J. Wood, C. Rascón, Wedge filling, cone filling and the strong-fluctuation regime. *J. Phys. Condens. Matter* **13**, 4519–4613 (2001).

47. K. Rejmer, S. Dietrich, M. Napiórkowski, Filling transition for a wedge. *Phys. Rev. E* **60**, 4027–4042 (1999).

48. P. G. Debenedetti, *Metastable Liquids* (Princeton Univ. Press, 1997).

49. R. Seemann, M. Brinkmann, S. Herminghaus, K. Khare, B. M. Law, S. McBride, K. Kostourou, E. Gurevich, S. Bommer, C. Herrmann, D. Michler, Wetting morphologies and their transitions in grooved substrates. *J. Phys. Condens. Matter* **23**, 184108 (2011).

50. S. Puri, K. Binder, Surface effects on kinetics of ordering. *Z. Phys. B* **86**, 263–271 (1992).

51. H. Tanaka, Interplay between wetting and phase separation in binary fluid mixtures: Roles of hydrodynamics. *J. Phys. Condens. Matter* **13**, 4637–4674 (2001).

Science Advances

Impact of surface roughness on liquid-liquid transition

Ken-ichiro Murata and Hajime Tanaka

ARTICLE TOOLS	http://advances.sciencemag.org/content/3/2/e1602209
SUPPLEMENTARY MATERIALS	http://advances.sciencemag.org/content/suppl/2017/02/13/3.2.e1602209.DC1
REFERENCES	This article cites 50 articles, 3 of which you can access for free http://advances.sciencemag.org/content/3/2/e1602209#BIBL
PERMISSIONS	http://www.sciencemag.org/help/reprints-and-permissions

Use of this article is subject to the Terms of Service